KINETIC STUDY ON THE REMOVAL OF HEAVY METALS BY CAJANUS CAJAN HUSK AND BUTEA MONOSPERMA LEAVES

Mallappa A. Devani [a], Basudeb Munshi [b*]

[a] *Department of Chemical Engineering, Bheemanna Khandre Institute of Technology, Bhalki 585328, Karnataka, India*

[b] *Department of Chemical Engineering, National Institute of Technology, Rourkela 769008, Odisha, India*

*Corresponding author. E-mail: basudeb@nitrkl.ac.in

Abstract

The removal of heavy metals from wastewater has become crucial to meet safe discharge standards. Development of more economic process has been strived owing to high cost of adsorbents. Thus, biosorption process has become the area of interest to researchers and engineers. The present study has carried out the transient removal of heavy metals from wastewater by both physically treated and chemically modified *Cajanus cajan* (Pigeon pea) husk (CCH) as novel biosorbents. Work includes five different models such as first order, second order, n^{th} order, first order reversible and second order reversible under the heading of prediction of transient concentration of metal in the solution are used, and under the heading of prediction of transient metal uptake capacity; fractional power, pseudo first order, pseudo second order, second order reversible, Elovich, intra-particle diffusion and film diffusion models are used to analyse the kinetic data. For a metal at any particular initial concentration the best kinetic model with the least RMSE is identified. Pictorial comparison between experimental and pseudo second order and pseudo first order model predictive data of Cd(II) and Cu(II) transient biosorption, respectively onto CCH are illustrated . The trend of the results shows a successful prediction capability of all the kinetic models used in the present work. According to RMSE data, it can be concluded that the best kinetic models are pseudo second order for Cd(II) and pseudo first order for Cu(II). It has been found that the required equilibrium time is always less for the chemically activated than the physically activated sorbent. At 100 mg/L initial metal concentration, pseudo-first-order model has been identified as the best kinetic model for the transient Cu(II) and the best kinetic model for fitting the transient sorption of Cd(II) on CCH is pseudo-second-order. At initial metal concentration of 150 mg/L, initial biosorption rate of 9.7038 for Cd(II) on CCH(N) is greater than 1.4553 for Cu(II) on CCH(N). These indicate that Cd(II) undergoes faster adsorption rate than Cu(II) onto CCH

Keywords: Biosorption, Cadmium(II), Copper(II), Kinetics

Abbreviations

CCH	Cajanus cajan husk
CCH(N)	physically activated Cajanus cajan husk
CCH(CA)	Chemically activated Cajanus cajan husk

1. Introduction

Among all the pollutants, heavy metals are considered to be hazardous even at low concentrations because of their carcinogenic properties like non-biodegradability and bio-accumulation [1]. Their peril is multiplied by their buildup in the environment through the food chain. All metal processing actions lose and/or release sometimes even huge amount of heavy metals. The release of such heavy metals into aquatic ecosystems has become a major concern in India and other industrially developing nations. As a consequence of the various industrial activities, the respective wastewater effluents contain such heavy metals and enter the aquatic systems in significant quantities due to the lack of sufficient treatment plants and technologies.

The improvement and achievement of cost-effective process such as biosorption process for the removal of the heavy metals is crucial in order to improve the competitiveness of industrial processing operations and to decrease the environmental hazard of toxic metal containing wastewater. Knowledge on the controlling mechanism of the biosorption processes such as chemical reactions, diffusion control and mass transfer is vital for designing the biosorption process. The desirable quick kinetics has considerable realistic significance as it makes the volume of reactor smaller with higher efficiency and economy.

The kinetic models in general describe the mechanism and order of reaction in biosorption systems. Present work intends to select the most suitable kinetic model out of twelve tested models to predict the biosorption kinetics experimental data of Cd(II) and Cu(II) biosorption on *Cajanus cajan* husk in their physically treated and chemically activated form. The used initial concentrations of metals are 100 and 150 mg/L. *Cajanus cajan* husk was selected as it is inexpensive and easily available source of biomass in the local area.

2. Materials and Methods

2.1. Chemicals and instruments

Cadmium nitrate [$Cd(NO_3)_2.4H_2O$] was used to prepare Cd(II) and Copper (II) sulphate-5-hydrate [$CuSO_4.5H_2O$] was used to prepare Cu(II) solutions in distilled water. Along these, sodium hydroxide, hydrochloric acid, calcium chloride and ethanol were also used in the current experimental study. All the

chemicals provided by SD Fine Chemicals, Mumbai and used for the chemical activation of the *Cajanus cajan* husk were of analytical grade.

The instruments used were: a precision electronic weighing balance (Essae Teraoka Ltd.), orbital shaker (Kemi, Kerala, India), atomic absorption spectrophotometer (Elico-167 model, India), hot air oven (Kemi, Kerala, India), and pH meter (Elico-LI 612 model).

2.2. Preparation of biosorbents

The *Cajanus cajan* husk was ground in a mixer-grinder and boiled in water four times to remove the color. It was then dried in a hot air oven at 85 °C for 24 h and the dried material was screened and the size fraction of average size, 0.5125 mm was stored in airtight polythene bags and designated as CCH(N).

For chemical activation, 500 mL absolute ethanol, 250 mL 0.5 mol/L NaOH and 250 mL of 1.5 mol/L $CaCl_2$ were added to 100 g of the above physically prepared husk, mixed thoroughly and kept aside for 24 h. The supernatant liquid was drained out and the husk was thoroughly washed with distilled water to remove the residual chemicals and designated as CCH(CA).

2.3. Kinetic studies

0.5 g of the above prepared husk, CCH(N) and CCH(CA), was added to a series of 250 mL glass beakers containing 50 mL of 100 / 150 mg/L Cd(II) as initial concentrations and shaken at 180 rpm. Samples were quickly vacuum filtered at time intervals of 0.5, 1, 3, 6, 10, 25, 45, 60, 75 and 90 minutes intervals and the left over concentrations of Cd(II) were determined by atomic absorption spectrophotometer to estimate the metal uptake q_t (mg/g) at any time *t*. Mathematical expression of it is

$$q_t = \frac{(C_0 - C_t)}{m/V} \quad (1)$$

where, C_0 and C_t are initial concentration and momentary concentration at time *t* of the metal in solution (mg/L), *m* is the bio-sorbent mass (g) and *V* is the volume of the solution (L). Origin Pro 8 software has been used for the non-linear curve fitting of the experimental data to the kinetic models.

3. Results and discussions

3.1 The transient metal uptakes

The transient metal uptakes of both CCH at two different sorbate concentrations in solution are given in Fig. 1 and Fig. 2. The trend of the transient metal uptake is just opposite of the metal concentration in the solution. The figures show that the initial increase of the uptake capacity is high and it becomes slow with time as approaches the equilibrium state. It is depicted that the most of the biosorption of Cd(II) and Cu(II) takes place within first 20 to 30 min. The figures also show after equilibrium state further

treatment for more duration does not alter the capacity of the biosorption. The equilibrium times for the batch biosorption processes are given in Table 1. According to the equilibrium time data, in the table, the Cd(II) on CCH biosorption process is the fastest and Cu(II) on CCH is the slowest. The data of the equilibrium sorption capacity for both the metals and biosorbents are also given in the table. In general the required equilibrium time, t_e for C_o = 150 mg/L is less than or equal to the t_e required for C_o = 100 mg/L. This occurs due to the presence of higher driving force for metal transport from solution to the sorbent surface at higher initial concentration of metals. The required equilibrium time is always less for the chemically than the physically activated sorbent. It arises due to the presence of active sites having carboxylic functional group in CCH(CA), which makes the metal transport for the CCH(CA) more irreversible than CCH(N). Higher decrease of t_e between physically and chemically activated CCH is observed at higher concentration. The metal ion concentration difference between the solution and sorbent surface may be the prime reason behind it. The table also shows that the equilibrium uptake capacity which is achieved after long operational time increases with the initial metal concentration in all the cases. The reason behind this is the availability of the unsaturated active sites at lower initial concentration of metals which get filled at higher concentration level of metals.

Table 1 Equilibrium time and equilibrium metal sorption capacity of CCH

Metal	**Biosorbent**	**C_o (mg/L)**	**Equilibrium time t_e (min)**	**Equilibrium uptake q_e (mg/g)**
Cd(II)	CCH(N)	100	25	8.390
		150	22	13.36
	CCH(CA)	100	20	9.980
		150	15	14.25
Cu(II)	CCH(N)	100	35	7.997
		150	35	13.71
	CCH(CA)	100	30	9.280
		150	25	13.15

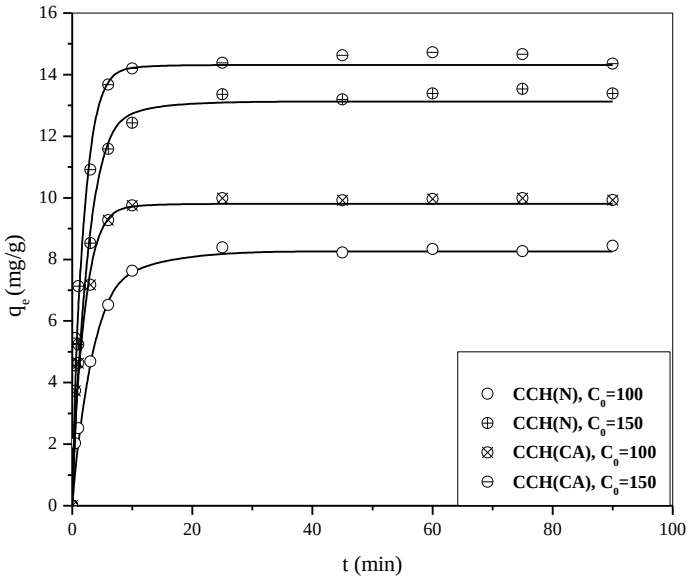

Fig. 1 The transient metal uptake capacity of Cd(II) onto CCH at 303.15 K, pH 6.0 and dosage 0.5 g

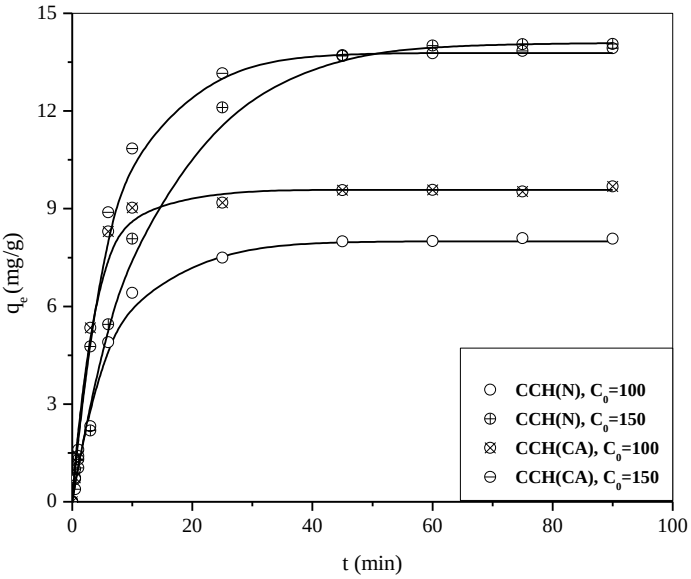

Fig. 2 The transient metal uptake capacity of Cu(II) onto CCH at 303.15 K, pH 5.5 and dosage 0.5 g

3.2 Fitting of transient metal concentration in solution

A particular amount of biosorbent has a certain maximum metal sorption capacity. Hence, the dynamic sorbent capacity is surely affected by the initial metal concentrations.

In this section, different irreversible models are selected and solved to predict the transient concentration profiles of metal ions. The comparison between the predicted and the experimental equilibrium metal concentrations are also discussed here.

3.2.1 First order model

The first order model equations for a metal ion in differential forms [2] are given below.

$$\frac{dC_t}{dt} = -k_f C_t \quad (2)$$

Using the initial condition, $C_t = C_0$ at $t = 0$, the integrated time dependent metal concentration is expressed as

$$C_t = C_0 \exp(-k_f t) \quad (3)$$

Rearrangement of Eq. 3 gives

$$ln\frac{C_t}{C_0} = -k_f t \quad (4)$$

In the model, C_o and C_t are the initial and momentary concentrations of metal (mg/L), and k_f is the first order rate constant, (l/min.) [3].

The estimated k_f values along with the R^2 and RMSE values for different biosorption systems are given in Table 2. The value of the k_f signifies the rate of biosorption. So, based on k_f it can be concluded that in general chemically activated sorbent is more favorable.

The values of R^2 and RMSE indicate that the first order model approximation is insufficient to predict the transient metal concentration profiles in solution.

In all the cases the estimated rate constants for chemically activated biosorbents is higher than that of normal biosorbents. It is because of the presence of the active functional groups on the chemical activated biosorbents surface than the physically activated sorbents.

Table 2 Kinetic parameter values for the biosorption of Cd(II) and Cu(II) on CCH at 303.15 K

S. No.	Model	Metal	Biosorbent	C_0 (mg/L)	Parameter values	R^2	RMSE
1	First order	Cd(II)	CCH(N)	100	$\boldsymbol{k_f}$ = 0.0275	0.729	29.966
				150	$\boldsymbol{k_f}$ = 0.0343	0.717	50.854
			CCH(CA)	100	$\boldsymbol{k_f}$ = 0.0857	0.784	30.737
				150	$\boldsymbol{k_f}$ = 0.0547	0.680	55.100
		Cu(II)	CCH(N)	100	$\boldsymbol{k_f}$ = 0.0244	0.826	21.583

				150	k_f = 0.0388		0.960	16.551
			CCH(CA)	100	k_f = 0.0481		0.700	28.853
				150	k_f = 0.0378		0.833	31.668
2	Second order	Cd(II)	CCH(N)	100	k_s = 0.0008		0.845	19.996
				150	k_s = 0.0008		0.847	31.427
			CCH(CA)	100	k_s = 0.0573		0.793	18.455
				150	k_s = 0.0037		0.968	13.207
		Cu(II)	CCH(N)	100	k_s = 0.0006		0.918	13.019
				150	k_s = 0.0130		0.960	15.239
			CCH(CA)	100	k_s = 0.0035		0.968	7.7507
				150	k_s = 0.0011		0.983	8.6700
3	n^{th} order	Cd(II)	CCH(N)	100	k_n = 0.0005	n = 2.2	0.881	13.205
				150	k_n = 0.0007	n = 2.1	0.883	25.406
			CCH(CA)	100	k_n = 0.0302	n = 1.6	0.989	3.1076
				150	k_n = 0.0019	n = 2.5	0.964	10.146
		Cu(II)	CCH(N)	100	k_n = 0.0002	n = 2.5	0.974	5.4154
				150	k_n = 0.0020	n = 1.8	0.982	9.2245
			CCH(CA)	100	k_n = 0.0035	n = 2.0	0.968	7.7507
				150	k_n = 0.0070	n = 2.2	0.986	8.3788
4	First order reversible	Cd(II)	CCH(N)	100	k_1 = 0.0245	k_2 = 0.0516	k_D = 0.4747	0.991	0.3295
				150	k_1 = 0.0382	k_2 = 0.0544	k_D = 0.7071	0.977	0.7600
			CCH(CA)	100	k_1 = 0.0589	k_2 = 0.0115	k_D = 5.1250	0.980	0.4922
				150	k_1 = 0.0628	k_2 = 0.0299	k_D = 2.0960	0.983	1.6579
		Cu(II)	CCH(N)	100	k_1 = 0.0120	k_2 = 0.0301	k_D = 0.3992	0.993	0.2636
				150	k_1 = 0.0076	k_2 = 0.0048	k_D = 1.5560	0.997	0.3057
			CCH(CA)	100	k_1 = 0.0258	k_2 = 0.0113	k_D = 2.2790	0.992	0.3716
				150	k_1 = 0.0139	k_2 = 0.0123	k_D = 1.1300	0.996	0.4081

3.2.2 Second order model

The rate of second order reactions is proportional to the product of concentrations of two reactants [2]. The transient second order ordinary differential equation of metal in solution is

$$\frac{dC_t}{dt} = -k_S C_t^2 \quad (5)$$

The integration of the above equation using the initial condition, $C_t = C_0$ at $t = 0$ gives Eq. 5 containing the variation of C_t with time, t.

$$C_t = \frac{C_0}{(C_0 k_s t + 1)} \quad (6)$$

where, k_s is the second order rate constant, (g/mg min).

For different systems the calculated values of k_s are tabulated in Table 2. The tabulated data show that like k_f, k_s is also higher for the chemically activated biosorbents except Cu(II) sorption on CCH(CA) with initial concentration of 150 mg/L. According to the k_s values, the rate of Cd(II) biosorption is higher than Cu(II). The extent of ion association increases with increasing the size of the ion that helps to form ion triplet in solution. The interaction of ion triplet is more favorable than the individual ions. Thus, overall, k_s follows the order of Cd(II) > Cu(II), which is according to the order of the sizes of the ions. The predicted concentration profiles following the second order kinetic equation are compared with the experimental data. The comparison shows that second order model also fails to predict the experimental kinetic data. It is because the influence of chemical reactions and transport phenomena are inseparable.

The same observations are also reflected in R^2 and RMSE values. It is therefore concluded that the kinetics of the biosorption in the present study cannot be represented satisfactorily by the second order reaction.

3.2.3 n^{th} order model

The final transient concentration profile equation for n^{th} order reaction is:

$$\frac{C_t^{n-1}}{C_0^{n-1}} = \frac{1}{1+k_n(n-1)C_0^{n-1}t} \quad (7)$$

where, k_n is the n^{th} order rate constant, (g/mg.min). For different systems the values of k_n are calculated for the optimum n which produce the minimum error between the predicted and experimental kinetic data. The tabulated data in Table 2 show that like first order rate constant, k_f and second order rate constant, k_s, k_n is also higher for the chemically activated biosorbents. Based on low R^2 and high RMSE values given in the table, it can be stated that the n^{th} order model is an unsuccessful kinetic model.

3.3 Fitting of transient metal uptake capacity of biosorbents

As concentration of metal in solution changes with time, the biosorption capacity also shows the transient behaviour. Thus, it is necessary and useful to model the transient metal uptake capacity of different biosorbents. In the present work, some selected conventional kinetic models are used for studying the kinetic behaviour of the metal uptake of the biosorption process.

3.3.1 Reversible models

In the reversible models, the forward reaction occurs between the metal ion and active site, and the backward reaction involves with the degradation of metal ion-active site complex. Two reversible models namely first order and second order are included in the current section.

3.3.1.1 First order reversible model

The following equation represents the transient mass balance equation for reversible reaction system with k_1 and k_2 as the forward and backward rate constants.

$$\frac{dq_t}{dt} = k_1 C_t - k_2 q_t \tag{8}$$

Substituting q_t in terms of C_t and using $C_t = C_o$ at t = 0 as the initial concentration the derived transient expression of C_t is obtained as

$$\frac{C_t}{C_0} = \frac{1}{k_D\frac{m}{V}+1} + \left(1 - \frac{1}{k_D\frac{m}{V}+1}\right)\exp\left[-\left(\frac{k_D k_2 m}{V} + k_2\right)t\right] \tag{9}$$

in which $k_D = k_1/k_2$.

For different systems, the values of k_1, k_2 and k_D are calculated through non-linear data fitting models available in MATLAB 2013a to minimize the error between the experimental and model's kinetic data. The R^2 and RMSE values for all the cases are calculated and tabulated in Table 2. The graphical comparison (corresponding figure not reported here), reasonably high R^2 and low RMSE values find first order reversible as the moderately good kinetic model.

The tabulated data show that k_1 for chemically activated sorbent is higher than the physically activated sorbent. It occurs due to higher reactivity of active sites on the chemically activated sorbents. The k_2 values for the physically activated sorbents are greater than the chemically activated sorbents except for Cu(II) sorption on CCH at higher initial metal concentration. In any system, the higher values of equilibrium concentration, C_e results in lower k_1 and vice versa. Similarly k_2 becomes high for lower equilibrium sorbent capacity, q_t. Simultaneous higher values of k_1 and lower values of k_2 are responsible for the lower biosorption capacity of the biosorbents. In general, it is observed in the table that $k_1 > k_2$ i.e. $k_D > 1.0$ for the chemically activated biosorbents and a reverse trend, i.e. $k_D < 1.0$ for physically activated biosorbents. The increase of C_e and simultaneous decrease of q_t with increase of the initial metal concentration are responsible to obtain $k_D > 1.0$ for the sorption of Cu(II) on CCH(N).

3.3.1.2 Second order reversible model

The interaction that occurs between a metal and biosorbents in a solution can be represented by a second order reversible reaction

$$M + A \rightleftharpoons MA \tag{10}$$

in which *M* is the metal ion in the solution, *A* is the biosorption site on the surface of the biosorbent and *MA* is the metal-sorbent complex.

The rate of metal uptake [4] by the biosorbents is

$$\frac{dq_t}{dt} = k_1 C(q_e - q_t) - k_2 q_t \quad (11)$$

where, q_t and C stands for metal concentration in the solid and solution at time t, and k_1 and k_2 are the forward and backward rate constants.

On integration of the Eq. 11 with initial conditions and applying mass balance gives

$$\frac{C}{C_0} = 1 - \frac{1}{C_0}\frac{m}{v}\frac{(b+a)\left[1-exp\left(2a\frac{m}{v}k_1 t\right)\right]}{\left[\frac{(b+a)}{(b-a)} - \exp\left(-2a\frac{m}{v}k_1 t\right)\right]} \quad (12)$$

$$a^2 = b^2 - C_0 q_e \frac{v}{m} \quad (13)$$

$$b = 0.5\left(C_0\frac{v}{m} + q_e + k_D\frac{v}{m}\right) \quad (14)$$

where, $k_D = {k_2}/{k_1}$

For different systems the values of k_1 and k_D are calculated by fitting the above equation to the experimental kinetic data and tabulated in Table 3. Higher values of k_1 are obtained for chemically activated biosorbents in all the cases. Being a product small magnitude k_1 and k_D, the k_2 values are very low. Thus, it can be concluded here that the rate of the degradation of sorbate-active site complex are negligible as compared to the forward rate of complex formation. Unlike first order reversible, the forward rate constant in case of second order reversible model does not follow a particular trend with the change of initial metal concentration. It is because the k_1 in second order model is the coefficient of a highly non-linear term, product of equilibrium metal and unused active sites concentrations. Similarly, k_D i.e. in turn k_2 also does not follow a particular trend with C_o.

Table 3 Kinetic parameter values for the biosorption of Cd(II) and Cu(II) on CCH at 303.15 K

S. No.	Model	Metal	Biosorbent	C_0 (mg/L)	Parameter values			R^2	RMSE
5	Second order reversible	Cd(II)	CCH(N)	100	$\boldsymbol{k_1}$ = 0.0023	$\boldsymbol{k_D}$ = 0.8199		0.972	0.8936
				150	$\boldsymbol{k_1}$ = 0.0046	$\boldsymbol{k_D}$ = 2.00×10^{-8}		0.990	0.4506
			CCH(CA)	100	$\boldsymbol{k_1}$ = 0.0107	$\boldsymbol{k_D}$ = 1.00×10^{-5}		0.989	0.3747
				150	$\boldsymbol{k_1}$ = 0.0073	$\boldsymbol{k_D}$ = 0.0001		0.993	0.4105
		Cu(II)	CCH(N)	100	$\boldsymbol{k_1}$ = 0.0021	$\boldsymbol{k_D}$ = 0.01		0.988	0.3560
				150	$\boldsymbol{k_1}$ = 0.0009	$\boldsymbol{k_D}$ = 0.002		0.984	0.9831
			CCH(CA)	100	$\boldsymbol{k_1}$ = 0.0043	$\boldsymbol{k_D}$ = 0.001		0.972	0.7602
				150	$\boldsymbol{k_1}$ = 0.0056	$\boldsymbol{k_D}$ = 0.01		0.989	0.8478
6	Fractional power	Cd(II)	CCH(N)	100	$\boldsymbol{k_F}$ = 3.8356	$\boldsymbol{\vartheta}$ = 0.1958	$\boldsymbol{k_F\vartheta}$ = 0.7510	0.898	0.9460
				150	$\boldsymbol{k_F}$ = 7.1212	$\boldsymbol{\vartheta}$ = 0.1609	$\boldsymbol{k_F\vartheta}$ = 1.1458	0.909	1.3505

			CCH(CA)	100	k_F = 5.9089	ϑ = 0.1356	$k_F\vartheta$ = 0.8012	0.894	1.0625
				150	k_F = 8.8114	ϑ = 0.1308	$k_F\vartheta$ = 1.1525	0.895	1.5341
		Cu(II)	CCH(N)	100	k_F = 2.4895	ϑ = 0.2872	$k_F\vartheta$ = 0.7149	0.909	0.9501
				150	k_F = 2.7797	ϑ = 0.3876	$k_F\vartheta$ = 1.0774	0.941	1.4112
			CCH(CA)	100	k_F = 3.9151	ϑ = 0.2264	$k_F\vartheta$ = 0.8863	0.821	1.6092
				150	k_F = 4.0676	ϑ = 0.3006	$k_F\vartheta$ = 1.2227	0.886	1.9253
7	Pseudo-first-order	Cd(II)	CCH(N)	100	q_e = 8.2600		k_1 = 0.2963	0.991	0.3251
				150	q_e = 13.128		k_1 = 0.4362	0.997	0.7559
			CCH(CA)	100	q_e = 9.8086		k_1 = 0.6007	0.980	0.4909
				150	q_e = 14.317		k_1 = 0.6581	0.983	0.6385
		Cu(II)	CCH(N)	100	q_e = 7.9969		k_1 = 0.1501	0.993	0.2625
				150	q_e = 14.094		k_1 = 0.0799	0.997	0.3055
			CCH(CA)	100	q_e = 9.5798		k_1 = 0.2691	0.992	0.3703
				150	q_e = 13.781		k_1 = 0.1517	0.996	0.4053

The calculated RMSE values are given in the table. The R^2 and RMSE of second order reversible model in some cases are lower and higher in other cases as compared to the R^2 and RMSE of the first order reversible models given in Table 3. The graphical observations (corresponding figure not reported here), R^2 and RMSE values also conclude that second order reversible model is also a moderately good model to fit the experimental kinetic data.

3.3.1.3 Fractional power model

This model indicates that the metal uptake capacity increases exponentially with time [5]. Mathematically it is expressed as

$$q_t = k_F t^{\vartheta} \tag{15}$$

where, q_t is the amount of metal adsorbed at any time t. k_F and ϑ are the coefficients to be evaluated from the transient sorption data. ϑ is usually less than unity for good fitting of the biosorption kinetic data into the fractional power model. k_F determines the equilibrium sorbent capacity, q_e. ϑ is a controlling parameter for the dynamic sorbent capacity, q_t. The product of the model constants i.e. $k_F\vartheta$ called the specific biosorption rate at time, t = 1.0.

The calculated k_F and ϑ values are given in Table 3. The estimated k_F values for the chemically activated biosorbents are usually higher than the physically activated biosorbents. The reason behind this is the

greater metal removal capacity of the chemically activated than the physically activated sorbents at equilibrium. Being a controlling parameter ϑ becomes less for the higher k_F system. Thus, for chemically activated biosorbents ϑ is less than the physically activated sorbents. The variation q_t with t shows that higher rate of initial sorbent capacity for chemically activated than the physically activated sorbents. The same observation is validated through the estimated values of the tabulated $k_F\vartheta$. For the chemically activated sorbents, $k_F\vartheta$ is appeared higher than the physically activated sorbents.

The estimated R^2 and RMSE values for different metals are also tabulated in the table. The comparison of estimated R^2 and RMSE values guide us to conclude that that the considered power law model is also moderately good for fitting the experimental kinetic data of different metals.

3.3.2 Irreversible models

The kinetic data of the biosorbent capacity can also be represented by irreversible kinetic model. According to it, the sorbate-sorbent complexes are stable and never undergo degradation during the biosorption process.

3.3.2.1 Pseudo-First-Order model in terms of active site concentration

The pseudo-first-order kinetic model is one of the most widely employed rate equation for evaluating the sorption of a sorbate from a liquid solution [6]. The kinetic performance is usually represented by pseudo-first-order rate model when biosorption of a solute from liquid is led by diffusion through a boundary layer [7]. This model is expressed mathematically as:

$$\frac{dq_t}{dt} = k_1(q_e - q_t) \tag{16}$$

Integration of Eq. 16 with initial condition $q_t = 0$ at $t = 0$ gives Eq. 17.

$$q_t = q_e(1 - e^{-k_1 t}) \tag{17}$$

where, q_e is the solute biosorbed at equilibrium (mg/g), q_t is the solute biosorbed at any time t, and k_1 is the first order rate constant (sec^{-1}).

The estimated values of k_1 for both 100 and 150 mg/L initial concentrations with both CCH and BMLP biosorbents are tabulated in Table 3. The estimated q_e shown in the tables for all the metal sorption are matching excellently with the experimental equilibrium sorbent capacities given in the Table 1. In all the cases, the pseudo-first-order reaction rate constant, k_1 are observed higher for the chemically activated sorbents.

The results confirmed that the pseudo-first-order model well predicts the transient biosorbent capacity profile for CCH as biosorbent. For the biosorption of Cu(II) on CCH, the kinetic data is best fitted with pseudo-first-order model with very high R^2 and low RMSE values. A reasonably good fitting of the experimental data to the pseudo-first-order kinetic model with low RMSE values for Cd(II) sorption on CCH(N) at both C_o = 100 and 150 mg/L and on CCH(CA) only at C_o = 150 mg/L are observed. Overall, high R^2 and low RMSE values in the tables suggest that the pseudo-first-order model is an efficient model.

3.3.2.2 Pseudo-Second-Order model in terms of active site concentration

Pseudo-second-order model is established on the hypothesis that biosorption pursue second-order chemisorption. The differential equation for the pseudo-second-order model is

$$\frac{dq_t}{dt} = k_2(q_e - q_t)^2 \quad (18)$$

where, k_2 (g/mg.sec) is the second order rate constant.

On integration of Eq.18 with initial condition $q_t = 0$ at $t = 0$, the transient model for q_t, [8] becomes

$$q_t = \frac{q_e^2 k_2 t}{1 + k_2 q_e t} \quad (19)$$

The values of the model constants are given in Table 4. The computed values of q_e using Eq. 19 are found very close to the experimental q_e given in Table 1. Thus, pseudo-second-order kinetic model predicts very well the equilibrium sorbent capacity. k_2 measures the rate of biosorption. The variations of k_2 with the type of metal and sorbents, and its related physical explanations are similar to the trend of k_1, rate constant for pseudo-first-order kinetics. The declining trend of k_2 with the rising of the initial metal concentration may be clarified by the decreasing rate of diffusion through the pores of the biosorbent surfaces.

Table 4 Kinetic parameter values for the biosorption of Cd(II) on CCH at 303.15 K

S. No.	Model	Metal	Biosorbent	C_0 (mg/L)	Parameter values			R^2	RMSE
8	Pseudo-second-order	Cd(II)	CCH(N)	100	$\boldsymbol{q_e}$ = 8.7380	$\boldsymbol{k_2}$ = 0.0529	$\boldsymbol{h}$ = 4.0398	0.991	0.2653
					$\boldsymbol{SR_{50}}$ = 1.0090	$\boldsymbol{SR_{90}}$ = 0.0403	$\boldsymbol{t_{1/2}}$ = 2.1631		
				150	$\boldsymbol{q_e}$ = 13.793	$\boldsymbol{k_2}$ = 0.0510	$\boldsymbol{h}$ = 9.7038	0.989	0.4554
					$\boldsymbol{SR_{50}}$ = 2.4259	$\boldsymbol{SR_{90}}$ = 0.0970	$\boldsymbol{t_{1/2}}$ = 1.4214		
			CCH(CA)	100	$\boldsymbol{q_e}$ = 10.263	$\boldsymbol{k_2}$ = 0.0938	$\boldsymbol{h}$ = 9.879	0.990	0.3119

					SR_{50} = 2.469	SR_{90} = 0.0988	$t_{1/2}$ = 1.0380		
				150	q_e = 14.982	k_2 = 0.0691	h = 15.512	0.993	0.3592
					SR_{50} = 3.8779	SR_{90} = 0.1551	$t_{1/2}$ = 0.9658		
		Cu(II)	CCH(N)	100	q_e = 8.8013	k_2 = 0.0219	h = 1.696	0.986	0.3519
					SR_{50} = 0.0424	SR_{90} = 0.0169	$t_{1/2}$ = 5.1880		
				150	q_e = 16.570	k_2 = 0.0053	h = 1.4553	0.991	0.5009
					SR_{50} = 0.3638	SR_{90} = 0.0145	$t_{1/2}$ = 11.386		
			CCH(CA)	100	q_e = 10.278	k_2 = 0.0356	h = 3.7601	0.969	0.6902
					SR_{50} = 0.9402	SR_{90} = 0.0376	$t_{1/2}$ = 2.7328		
				150	q_e = 15.226	k_2 = 0.0124	h = 2.8748	0.987	0.6930
					SR_{50} = 0.7187	SR_{90} = 0.0287	$t_{1/2}$ = 5.2963		
9	Second order model in terms both metal concentration in solution and sorbent	Cd(II)	CCH(N)	100	k_3 = 0.0021			0.988	0.3579
				150	k_3 = 0.0046			0.990	0.3753
			CCH(CA)	100	k_3 = 0.0108			0.989	0.4506
				150	k_3 = 0.0108			0.993	0.4105
		Cu(II)	CCH(N)	100	k_3 = 0.0021			0.988	0.3579
				150	k_3 = 0.0009			0.984	0.9820
			CCH(CA)	100	k_3 = 0.0043			0.972	0.7626
				150	k_3 = 0.0015			0.989	0.8467
10	Elovich	Cd(II)	CCH(N)	100	α_e = 23.726	β_e = 0.9149	R_E = 0.1302	0.942	0.4003
				150	α_e = 158.82	β_e = 0.8356	R_E = 0.0895	0.940	1.0443
			CCH(CA)	100	α_e = 179.63	β_e = 0.9507	R_E = 0.1053	0.924	0.8538
				150	α_e = 592.57	β_e = 0.8590	R_E = 0.0816	0.921	1.2496
		Cu(II)	CCH(N)	100	α_e = 6.4385	β_e = 0.8368	R_E = 0.1494	0.958	0.6394
				150	α_e = 5.7702	β_e = 0.6436	R_E = 0.1133	0.971	0.8572
			CCH(CA)	100	α_e = 17.163	β_e = 0.8283	R_E = 0.1300	0.885	1.2403
				150	α_e = 12.450	β_e = 0.6923	R_E = 0.1098	0.941	1.2918

The initial biosorption rate, h (mg/g/min) determined by Eq. 20 has been extensively used for the assessment of the biosorption rates [9].

$$h = \frac{dq_t}{dt}\Big|_{t=0} = k_2 q_e^2 \tag{20}$$

The initial biosorption rate, h is affected by the types of biosorbents. The above expression, is derived from Eq. 19. Further, the instantaneous rates (mg/g/min) at 50% (SR_{50}) and 90% (SR_{90}) of the sorbent capacity are obtained from pseudo-second-order rate equation.

$$SR_{50} = k_2[q_e - 0.5q_e]^2 = \frac{k_2 q_e^2}{4} = \frac{h}{4} \tag{21}$$

$$SR_{90} = k_2[q_e - 0.9q_e]^2 = \frac{k_2 q_e^2}{100} = \frac{h}{100} \tag{22}$$

The calculated SR_{50} and SR_{90} are presented in Table 4. The half-life ($t_{1/2}$) [8] of metal biosorption (the time at which half of the biosorption is accomplished and derived by substituting $q_t = q_e/2$ and $t = t_{1/2}$ in Eq. 19) is expressed by Eq. 23. $t_{1/2}$ is directly proportional to the biosorption ability of the biomass and inversely proportional to the initial biosorption rate:

$$t_{1/2} = \frac{1}{k_2 q_e} = \frac{q_e}{h} \tag{23}$$

As an illustrative example, at initial metal concentration of 100 mg/L, the $t_{1/2}$ values presented in Table 4 follow the order with Cu(II) on CCH(N) > Cu(II) on CCH(CA) > Cd(II) on CCH(N) > Cd(II) on CCH(CA). It shows that the biosorption of Cu(II) on CCH(N) is the slowest and Cd(II) on CCH(CA) is the fastest. The analysis also confirms that chemically activated biosorption is faster process than the physically activated sorbents. Moreover, based on the magnitude of h, SR_{50} and SR_{90} it is fair to conclude that with increasing the operation time the rate of change of sorbent capacity declines. It is due to the increasing rate of unavailability of active sites of the sorbent with the progress of the biosorption process.

The estimated biosorption rate constant, k_2 and equilibrium biosorption capacity, q_e, demonstrate a very good conformity with the pseudo-second-order equation having highest R^2 and lowest RMSE values. The estimated R^2 and RMSE values help to conclude that the pseudo-second model is an efficient model to fit the experimental kinetic data excellently.

3.3.2.3 Second-Order model in terms of both metal concentrations in solution and sorbent

There is a definite interaction between the metal ions in the solution and active site on the biosorbents. Giving importance to this interaction the reaction during the adsorption process can be written as

$$M + A \xrightarrow{k_3} MA \quad (24)$$

The second order rate expression of the above reaction follows Eq. 25

$$\frac{dc_t}{dt} = -k_3 c_t q_t \quad (25)$$

Eq. 25 is also an irreversible model and can be written in modified form as

$$\frac{dc_t}{dt} = -k_3 c_t (c_t - c_e) \quad (26)$$

where, k_3 (g/mg.sec) is the second order rate constant.

Integrating Eq. 26 using initial condition $c_t = c_o$ at $t = 0$ the metal concentration profile expression, Eq. 27 is deduced [4].

$$\frac{c_t}{c_0} = \frac{c_e}{c_0 - (c_0 - c_e)\exp(-k_3 c_e t)} \quad (27)$$

Further q_t is calculated by Eq. 1 using the computed c_t from Eq. 27.

Fitting values of the model parameter along with R^2 and RMSE are tabulated in Table 4. As usual like other kinetic models, the rate constant k_3 for the chemically activated sorbents are higher than the physically activated sorbents especially at higher initial concentration of the metals. Successful comparison of the fitting curves (corresponding figure not reported here) with the experimental kinetic data, reasonable high values of R^2 and low values of the RMSE confirm the suitability of the second order kinetic model in terms of both metal and active site concentrations.

3.3.2.4 Elovich kinetic model

This model presumes that the surface energetic sites of the biosorbents which control the sorption capacity are heterogeneous. It has limited use as it only explains the limiting condition eventually attained by the rate curve and is normally applied to explain the chemisorption kinetics of gases on the heterogeneous solid [10]. The model equation is

$$q_t = \ln(\alpha_e \beta_e t)^{1/\beta_e} \quad (28)$$

Constant α_e is associated to chemisorption rate and β_e is linked to the surface coverage. This model was used in the past to predict biosorption kinetics of some biomaterials [11, 12].

Substitution of the sorbent capacity $q = q_{ref,}$ at $t = t_{ref}$ in Eq. 28 results in

$$q_{ref} = \ln(\alpha_e \beta_e t_{ref})^{1/\beta_e} \quad (29)$$

Subtracting Eq. 29 from Eq. 28 the fractional sorption capacity q_t/q_{ref} can be written as

$$\frac{q_t}{q_{ref}} = \frac{1}{\beta_e q_e} ln\left(\frac{t}{t_{ref}}\right) \quad (30)$$

According to Wu et al. [13], the approaching equilibrium factor, R_E of the Elovich equation is defined as

$$R_E = \frac{1}{\beta_e q_e} \quad (31)$$

Including R_E Eq. 31 is rewritten as

$$\frac{q_t}{q_{ref}} = R_E ln\left(\frac{t}{t_{ref}}\right) \quad (32)$$

Depending on the nature of q_t/q_{ref} vs. t/t_{ref} plot, four zones are categorized based on the magnitude of R_E: if $R_E > 0.3$ (zone I), q_t/q_{ref} rises slowly; if $0.1 < R_E < 0.3$ (zone II), q_t/q_{ref} rises slightly faster; if $0.02 < R_E < 0.1$ (zone III), q_t/q_{ref} rises rapidly; if $R_E < 0.02$ (zone IV), q_t/q_{ref} instantly reaches the equilibrium sorbent capacity i.e. at $q_t/q_{ref} = 1.0$. In accordance to the equilibrium time data in Table 1, t_{ref} can be chosen as 35 min, the highest equilibrium time. At this t_{ref} the equilibrium sorbent capacities, q_e in Table 1 are taken as the q_{ref}. The computed R_E factor is listed in Table 4. R_E values identify the occurrence of Cd(II) sorption at lower initial metal concentration and Cu(II) sorption irrespective of the initial metal concentration at moderate rate in zone II. Being R_E in zone 3, the sorption of Cd(II) on CCH at higher initial metal concentration are quite rapid.

The estimated values of the model constants are tabulated in Table 4. The listed α_e shows that the sorption of metal on the chemically activated sorbent are more inclined to chemisorption type. The enlisted β_e in the tables accounts the surface coverage. The data in the table show that due to chemical activation the surface coverages are higher for the chemically activated than the physically activated sorbents. The comparisons of predicted and experimental data are qualitatively satisfactory. The quantitative comparison is carried out based on the R^2 and RMSE values given in the Table 4. The R^2 and RMSE values show a moderate prediction capability of the Elovich Kinetic Model as compared to pseudo-first-order and pseudo-second-order model.

3.3.3 Selection of the best kinetic model

From Table 5 it can be concluded that biosorption of Cd(II) on CCH is best fitted with pseudo-second-order model with the highest coefficient of determination, R^2 and lowest RMSE values.

The biosorption of Cu(II) on CCH is fitting by the pseudo-first-order model best having the highest R^2 and lowest RMSE. The tabulated R^2 and RMSE also show that first order reversible kinetic model is

equally competent with the pseudo-first-order model in case of Cu(II) removal by CCH(N) at C_o = 150 mg/L.

Table 5 R^{2}and RMSE values for kinetic models

Model	**P**	C_o = 100 mg/L				C_o = 150 mg/L			
		Cd(II) on CCH		**Cu(II) on CCH**		**Cd(II) on CCH**		**Cu(II) on CCH**	
		(N)	**(CA)**	**(N)**	**(CA)**	**(N)**	**(CA)**	**(N)**	**(CA)**
First-order	R^2	0.729	0.784	0.826	0.700	0.717	0.680	0.960	0.833
	RMSE	29.966	30.737	21.583	28.853	50.854	55.100	16.551	31.668
Second-order	R^2	0.845	0.793	0.918	0.968	0.847	0.968	0.960	0.983
	RMSE	19.996	18.455	13.019	7.7507	31.427	13.207	15.239	8.6700
nth order	R^2	0.881	0.989	0.974	0.968	0.883	0.964	0.982	0.986
	RMSE	13.205	3.1076	5.4154	7.7507	25.406	10.146	9.2245	8.3788
First order reversible	R^2	0.991	0.980	0.993	0.992	0.977	0.983	0.997	0.996
	RMSE	0.3295	0.4922	0.2636	0.3716	0.7600	1.6579	0.3057	0.4081
Second-order reversible	R^2	0.972	0.989	0.988	0.972	0.990	0.993	0.984	0.989
	RMSE	0.8936	0.3747	0.3560	0.7602	0.4506	0.4105	0.9831	0.8478
Fractional power	R^2	0.898	0.894	0.909	0.821	0.909	0.985	0.941	0.886
	RMSE	0.9460	1.0625	0.9501	1.6092	1.3505	1.5341	1.4112	1.9253
Pseudo-first-order	R^2	0.991	0.980	0.993	0.992	0.997	0.983	0.997	0.996
	RMSE	0.3251	0.4909	0.2625	0.3703	0.7559	0.6385	0.3055	0.4053
Pseudo-second-order	R^2	0.991	0.990	0.986	0.969	0.989	0.993	0.991	0.987
	RMSE	0.2653	0.3119	0.3519	0.6902	0.4559	0.3592	0.5009	0.6930
*Second-order	R^2	0.988	0.989	0.988	0.972	0.990	0.993	0.984	0.989
	RMSE	0.3579	0.4506	0.3579	0.7626	0.3753	0.4105	0.9820	0.8467
Elovich	R^2	0.942	0.924	0.958	0.885	0.940	0.921	0.971	0.941
	RMSE	0.4003	0.8538	0.6394	1.2403	1.0443	1.2496	0.8572	1.2918
Best fit model		Pseudo-second-order	Pseudo-second-order	Pseudo-first-order	Pseudo-first-order	Pseudo second-order	Pseudo second-order	Pseudo-first-order and First order reversible	Pseudo first-order

*Second-order in terms of both metal concentration in solution and sorbent, P - Parameter

3.3.4 Intra particle diffusion

In addition to the biosorption at outer surface of the sorbent due to active site, there is also a probability of intra-particle diffusion of metal ion from the outer surface into the pores of the sorbent material. Intra-particle diffusion is also called the homogeneous diffusion model in solid phase. For spherical particle of radius *R*, it can be represented as [14]

$$\frac{\partial q_t}{\partial t} = \frac{D_s}{r^2}\frac{\partial}{\partial r}\left(r^2 \frac{\partial q_t}{\partial r}\right) \quad (33)$$

in which *r* is the radial position and D_s is intra-particle diffusion coefficient.

3.3.4.1 Short time intra particle diffusion Model

Following the exact solution given by Crank [15], the simplified solution for short time with $q_t/q_e < 0.3$ is

$$\frac{q_t}{q_e} = 6\left(\frac{D_s}{R^2\pi}\right)^{1/2} t^{1/2} \quad (34)$$

From the above equation Weber and Morris [16] has concluded that uptake varies proportionate to $t^{1/2}$ over the complete time domain, and they proposed

$$q_t = k_{in}\sqrt{t} \quad (35)$$

in which k_{in} (mg/g/min$^{1/2}$) is the intra-particle diffusion constant.

From Eq. 34 and 35, we have

$$k_{in} = 6q_e\left(\frac{D_s}{R^2\pi}\right)^{1/2} \quad (36)$$

According to the Eq. 35 q_t vs. $t^{1/2}$ always pass through origin. It is true if the particle diffusion is only the rate controlling step. But sometimes the sorption kinetics is controlled by both intra-particle diffusion and external film diffusion, which will be discussed separately in the mass transfer coefficient section. Hence, the modified Weber-Morris model is given as

$$q_t = k_{in}\sqrt{t} + I \quad (37)$$

The intercept (I) gives an assessment of the width of the boundary layer, i.e., the bigger the I, greater is the boundary layer effect. It means the contribution of film diffusion to the metal transport from solution to the biosorbents increases with increasing I value. Applicability of the Eq. 37 indicates that the sorbent is porous and interconnected. Both the k_{in} and I can be evaluated by doing linear fitting of q_t vs. $t^{1/2}$ plot [17, 19, 20]. The variations of the transient biosorption capacity, q_t of the metals with $t^{1/2}$ are shown in Fig. 3 and Fig. 4. The plot is limited up to only equilibrium time, t_e; because t_e onwards there is negligible mass transport of metals to biosorbents and also the application of Eq. 34 is limited only for short time duration. The estimated intra particle diffusion constants are presented in Table 6. The fits are good for both Cd(II) and Cu(II) biosorption on physically treated and chemically activated CCH with coefficient of determination, R^2 values more than 0.9.

Table 6 Kinetic parameter values for the biosorption of Cd(II) on CCH at 303.15 K

S. No.	Model	Metal	Biosorbent	C_0 (mg/L)	Parameter values			R^2
11		Cd(II)	CCH(N)	100	$\boldsymbol{k_{in}}$ = 2.4688	$\boldsymbol{I}$ = 0.1712	$\boldsymbol{D_S}$ = 4.96×10^{-6}	0.9904

	Short time intra-particle diffusion			150	k_{in} = 3.9535	I = 1.0913	D_S = 5.01×10^{-6}	0.9949
			CCH(CA)	100	k_{in} = 3.0847	I = 1.1069	D_S = 5.47×10^{-6}	0.9322
				150	k_{in} = 4.4989	I = 1.7739	D_S = 5.71×10^{-6}	0.9161
		Cu(II)	CCH(N)	100	k_{in} = 2.0978	I = -0.5092	D_S = 3.94×10^{-6}	0.9543
				150	k_{in} = 2.5571	I = -0.8555	D_S = 1.99×10^{-6}	0.9087
			CCH(CA)	100	k_{in} = 3.3058	I = -0.8501	D_S = 7.27×10^{-6}	0.9359
				150	k_{in} = 3.8745	I = -1.5241	D_S = 4.97×10^{-6}	0.9336
12	Long-time intra-particle diffusion	Cd(II)	CCH(N)	100	k_{in}^{l}= 0.2485	I = 0.0867	D_S = $1.65\text{x}10^{-5}$	0.9964
				150	k_{in}^{l}= 0.2889	I = 0.1911	D_S = $1.92\text{x}10^{-5}$	0.9787
			CCH(CA)	100	k_{in}^{l}= 0.5018	I = 0.0418	D_S = $3.33\text{x}10^{-5}$	0.9910
				150	k_{in}^{l}= 0.4718	I = 0.1392	D_S = $3.14\text{x}10^{-5}$	0.9949
		Cu(II)	CCH(N)	100	k_{in}^{l}= 0.1128	I = 0.1248	D_S = 7.50×10^{-6}	0.9573
				150	k_{in}^{l}= 0.0723	I = 0.1039	D_S = 4.81×10^{-6}	0.9776
			CCH(CA)	100	k_{in}^{l}= 0.0883	I = 0.8261	D_S = 5.87×10^{-6}	0.7799
				150	k_{in}^{l}= 0.1149	I = 0.1153	D_S = 7.64×10^{-6}	0.9941

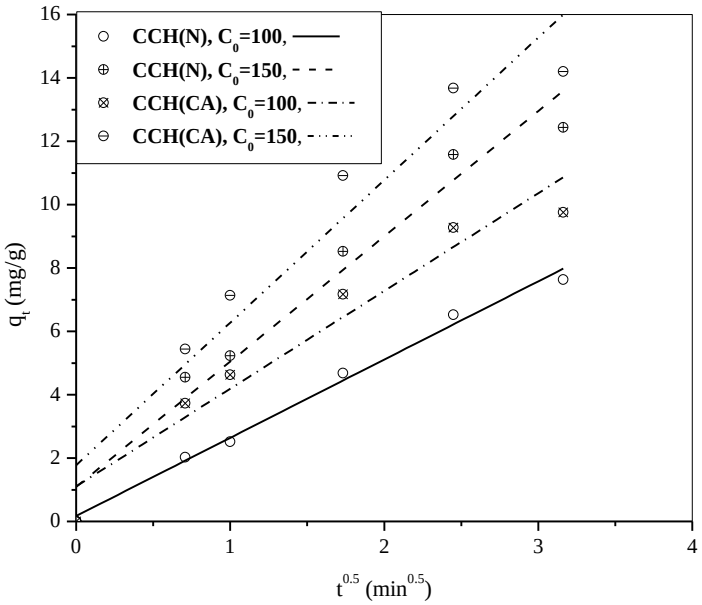

Fig. 3 Short time intra-particle diffusion plots for the biosorption of Cd(II) onto CCH at 303.15K, pH 6.0 and dosage 0.5g

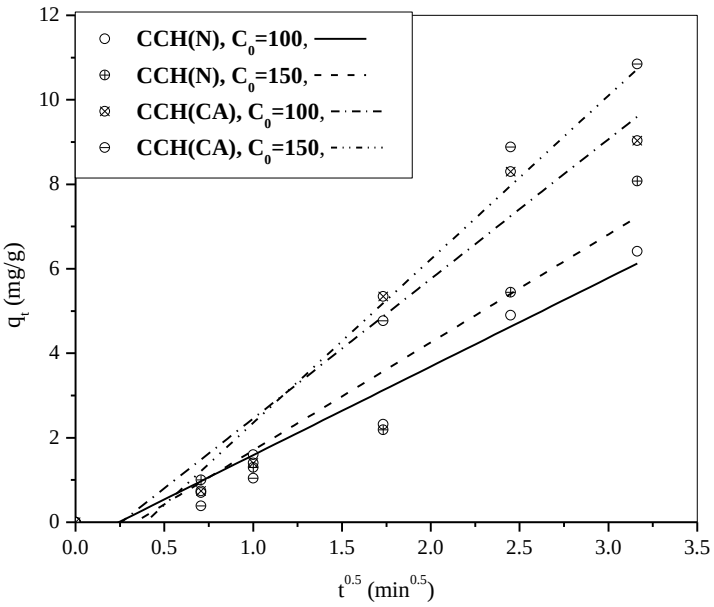

Fig. 4 Short time intra-particle diffusion plots for the biosorption of Cu(II) onto CCH at 303.15K, pH 5.5 and dosage 0.5g

It is confirmed from the Fig. 3 and Fig. 4 that the fitted straight lines are not passing through the origin suggesting that intra particle diffusion is not the sole rate controlling step for the biosorption of the metals studied on the biosorbents; there is also diffusional transport through the film. In all the cases the intra-particle diffusion constant, k_{in} are higher for chemically activated than physically activated sorbents. The biosorbents might have become more porous due to chemical activation. Thus, chemical activation favors the intra-particle diffusion metal transport along with the higher biosorption rate on the active surface. The calculated diffusion coefficient, D_S from Eq. 36 is also listed in the table.

3.3.4.2 Long-time intra particle diffusion model

For long time duration, the solution of Eq. 33 [21] can be written as

$$\ln\left[1-\frac{q_t}{q_e}\right]=-\frac{D_S\pi^2}{R^2}t+ln\frac{6}{\pi^2} \tag{38}$$

Above model can be expressed as:

$$-\ln\left[1-\frac{q_t}{q_e}\right]=k_{in}^{l}t+I \tag{39}$$

where, k_{in}^{l} (mg/g/min) is the intra-particle diffusion constant for long time duration. Comparing Eq. 38 and 39 we have,

$$k_{in}^{l}=\frac{\pi^2 D_S}{R^2} \tag{40}$$

From Eq. 40 the expression of diffusion coefficient, D_S (cm^2/min) can be written as

$$D_S=\frac{k_{in}^{l}R^2}{\pi^2} \tag{41}$$

q_t/q_e is the fractional ability of equilibrium. A linear plot of -ln(1−q_t/q_e) versus t with intercept I gives the k_{in}^{l} as the slope of the straight line. Using k_{in}^{l}, the intra-particle diffusion coefficient, D_S can also be determined by solving Eq. 41.

Fitting of the kinetic data of the biosorption of metals to the model Eq. 39 are shown graphically in Fig. 5 and Fig. 6 for different biosorbents. The calculated values of the model constants from the slope of the linear fittings are given in Table 6. The coefficient of determination, R^2, of the linear fitting lines are found to be greater than 0.9.

The linear nature of Eq. 39 confirms that the sorbents are porous in nature and interconnected. The magnitude of k_{in}^{l} determines the ease of mass transfer inside porous sorbent. The tabulated k_{in}^{l} as listed in

the table does not follow any particular trend with respect to the type of metal and sorbents, and initial metal concentration. The diffusional transport of Cd(II) appeared higher. Cu(II) has the lowest diffusing ability as compared to Cd(II). Further D_S are also calculated using long time intra-particle diffusion model i.e. solving Eq. 40. They are also enlisted in the table.

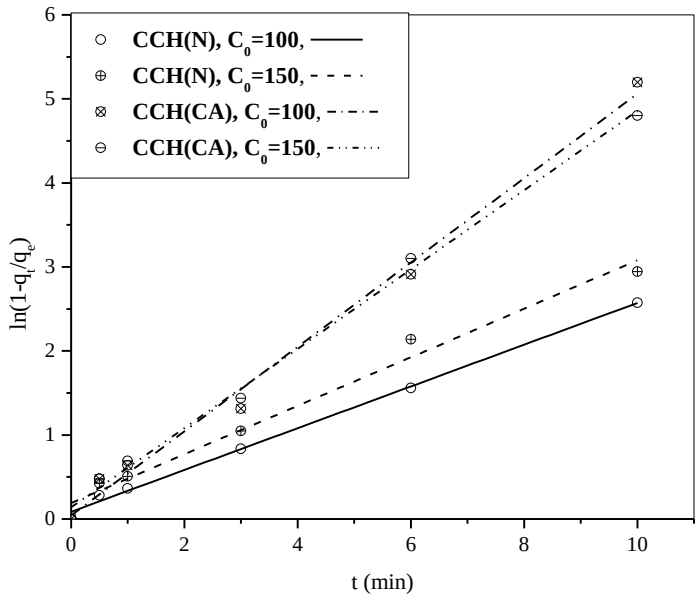

Fig. 5 Long time intra-particle diffusion plots for the biosorption of Cd(II) onto CCH at 303.15K, pH 6.0 and dosage 0.5g

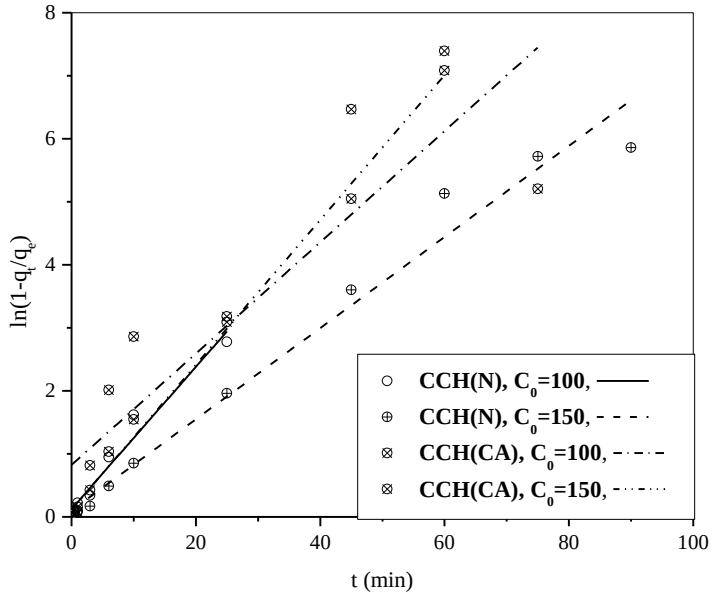

Fig. 6 Long time intra-particle diffusion plots for the biosorption of Cu(II) onto CCH at 303.15K, pH 5.5 and dosage 0.5g

The diffusion coefficients, D_s of the metal ions through the biosorbent particle are estimated following two methods namely short time and longtime intra-particle diffusion models. Those are tabulated in the Table 6. The data show that the calculated diffusion coefficients for Cu(II) ion are of the same order of magnitude in both the methods. In contrast, for other ions, the estimated D_s using long time method is higher than the short time method. Both the tables depict the dependency of D_s on initial metal concentration and type of biosorbent.

4. Conclusion

The following conclusions can be dawn in the kinetics study of the removal of Cd(II) and Cu(II) metal ions from wastewater:

- It has been found that the required equilibrium time is always less for the chemically activated than the physically activated sorbent.
- The transient Cd(II) and Cu(II) sorptions require 20 to 30 min to reach at equilibrium state.
- The best selected kinetic models are also found to depend on the type of metal and the initial metal concentration level in solution.
- At 100 mg/L initial metal concentration, pseudo-first-order model has been identified as the best kinetic model for the transient Cu(II) sorption on physically and chemically activated CCH. The best kinetic model for fitting the transient sorption of Cd(II) on CCH is pseudo second order.
- At 150 mg/L initial metal concentration, the best selected kinetic models are: pseudo- second-order for Cd(II) sorption on CCH, pseudo-first-order for Cu(II) sorption on CCH, first order and second order reversible for Cu(II) sorption on CCH(N) sorption on CCH(CA), respectively.
- The diffusion coefficients of the metals have been calculated using intra-particle diffusion models. The estimated diffusivities of the metals fall in the range of 10^{-7}-10^{-5} cm^2/min.

ORCID Id of authors

0000-0003-3824-1689

References

1. Cimino, G., Caristi, C. (1990) Acute toxicity of heavy metals to aerobic digestion of waste cheese whey. Biological Wastes, 33, 201–210.
2. Levenspiel, O. (2004). Chemical Reaction Engineering, 3rd edition, Wiley India Pvt. Ltd. New Delhi.
3. Eligwe, C.A., Okolue N.B. (1994) Adsorption of Iron(II) by a Nigerian brown coa. Fuel, 73, 569–572.
4. Chu, K.H., Hashim, M.A. (2003) Modeling batch equilibrium and kinetics of copper removal by crab shell. Separation Science and Technology, 38(16), 3927–3950.
5. Dalal, R.C. (1974) Desorption of phosphate by anion exchange resin. **Communication in Soil Science and Plant Analysis**, 5, 531–538.
6. Lagergren, S. (1898) Zur theorie der sogenannten adsorption gelster stoffe. Kungliga Svenska Vetenskapsakademiens. Handlingar, 24(4), 1–39.
7. Paresh, C., Sen Sarma, N., Sarma, H.P., (2010) Biosorption of cadmium(II) from aqueous solution using heartwood powder of Areca catechu. Chemical Engineering Journal, 162, 949–955.
8. Ho, Y.S. (2006). Review of second-order models for adsorption systems. Journal of Hazardous Materials, 136, 681–689.
9. Ho, Y.S., McKay, G. (1999) Pseudo-second order model for biosorption processes. Process Biochemistry, 34, 451–465.
10. Perez Marin, A.B., Aguilar, M.I., Meseguer, V.F., Ortuno, J.F., Saez, J., Llorens, M. (2009) Biosorption of chromium (III) by orange (Citrus cinensis) waste: Batch and continuous studies. Chemical Engineering Journal, 155, 199–206.
11. Ozacar, M., Sengil I.A. (2005) A kinetic study of metal complex dye adsorption onto pine sawdust. Process Biochemistry, 40, 565–572.
12. Cheung, C.W., Porter, J.F., McKay, G. (2001) Sorption kinetic analysis for the removal of Cadmium ions from effluents using bone char. Water Research, 35(3), 605–612.
13. Wu, F.C., Tseng, R.L., Juang, R.S. (2009) Characteristics of Elovich equation used for the analysis of adsorption kinetics in dye-chitosan systems. Chemical Engineering Journal, 150, 366–373.
14. Hui, Q., Lu, L., Bing-cai, P., Qing-jian, Z., Wei-ming, Z., Quan-xing, Z. (2009) Critical review in adsorption kinetic models. Journal of Zhejiang University SCIENCE A, 10(5), 716–724.
15. Crank, J. (1956) Mathematics of Diffusion. Oxford at the Clarendon Press, London, England.

16. Weber, W.J., Morris, J.C. (1963) Kinetics of adsorption on carbon from solution. Journal of Sanitary Engineering Division: American Society of Civil Engineers, 89(2), 31–60.
17. Ho, Y.S., McKay, G. (1998) Sorption of dye from aqueous solution by peat. Chemical Engineering Journal, 70, 115–124.
18. Srivastava, V.C., Mall, I.D., Mishra, I.M. (2006) Equilibrium modelling of single and binary adsorption of cadmium and nickel onto bagasse fly ash. Chemical Engineering Journal, 117, 79–91.
19. Goswami, S., Ghosh, U.C. (2005) Studies on adsorption behaviour of Cr(VI) onto synthetic hydrous stannic oxide. Water SA, 31, 597–602.
20. Morris, J.C., Weber, W.J. (1964) Removal of biologically-resistant pollutants from waste waters by adsorption, in: W. W. Eckanfelder (Ed.), Advances in Water Pollution Research, 2, Pergamon Press, London, 231–266.
21. Boyd, G.E., Adamson, A.M., Myers, L.S. (1949) The exchange adsorption of ions from aqueous solutions by organic zeolites. Journal of the American Chemical Society, 69, 2836–2842.